



Heterocyclic effect for optical properties of naphthoquinone-based pigment: 2-methyl-3-heteroarylthio-1,4-naphthalenedione



Akihiro Sako ^a, Koji Okuda ^a, Nobuo Tajima ^b, Reiko Kuroda ^c, Yoshitane Imai ^{a,*}

^a Department of Applied Chemistry, Faculty of Science and Engineering, Kindai University, 3-4-1 Kowakae, Higashi-Osaka, Osaka 577-8502, Japan

^b Computational Materials Science Center, National Institute for Materials Science, 1-2-1 Sengen, Tsukuba, Ibaraki, 305-0047, Japan

^c Research Institute for Science and Technology, Tokyo University of Science, 2641 Yamazaki, Noda-shi, Chiba, 278-8510, Japan

ARTICLE INFO

Article history:

Received 27 December 2016

Received in revised form

23 February 2017

Accepted 24 February 2017

Available online 27 February 2017

Keywords:

Chiral

Crystal structure

Heterocyclic

Naphthoquinone

Pigment

ABSTRACT

Three novel naphthoquinone-based heterocyclic pigments, 2-methyl-3-[(1-methyl-1H-imidazol-2-yl)thio-1,4-naphthalenedione], (4-methyl-4H-1,2,4-triazol-3-yl)thio-1,4-naphthalenedione, and (1-methyl-1H-tetrazol-5-yl)thio-1,4-naphthalenedione, are synthesized, and their optical properties in both solution and solid states are investigated. Depending on the heteroarylthio ring in the pigment, variation in optical properties is observed, e.g. characteristic colours for each pigment in the solution and solid states. The achiral pigment containing the 1-methyl-1H-tetrazol-5-yl ring exhibits a chiral space group and a CD signal in the solid state.

© 2017 Elsevier Ltd. All rights reserved.

1. Introduction

Organic dyes and pigments are among the most important useful organic materials for application as molecular colourants. In particular, functional organic dyes and pigments exhibiting various properties have attracted significant attention for applications as photomaterials because of their synergistic functionalities. Although several organic dyes and pigments have been developed thus far, few studies have reported the use of naphthoquinone derivatives as colourants.¹ Our group has reported the use of naphthoquinone pigments such as 2-methyl-3-arylthio-1,4-naphthalenedione as novel functional dyes and pigments.² Depending on the arylthio unit, naphthoquinone pigments previously reported exhibit unique optical properties such as characteristic colour and chiroptical properties in both solution and solid states. Thus far, the hydrocarbon aromatic ring has been used as an arylthio unit in naphthoquinone pigments. However, naphthoquinone pigments are not comprised of an additional thio unit instead of a hydrocarbon unit. To the best of our knowledge, another thio unit has been neither prepared nor investigated so far.

The synthesis of naphthoquinone pigments with heteroarylthio

units instead of hydrocarbon aryl units was attempted, and their characteristic multiple optical properties in solution and solid states were investigated. Three naphthoquinone-based heterocyclic compounds, 2-methyl-3-(1-methyl-1H-imidazol-2-yl)thio-1,4-naphthalenedione (**1**), 2-methyl-3-(4-methyl-4H-1,2,4-triazol-3-yl)thio-1,4-naphthalenedione (**2**), and 2-methyl-3-(1-methyl-1H-tetrazol-5-yl)thio-1,4-naphthalenedione (**3**), were synthesized as the target naphthoquinone pigments; these pigments have different heteroarylthio units (Fig. 1). In addition, 2-methyl-3-phenylthio-1,4-naphthalenedione (**4**) was synthesized as a reference compound, and its optical properties in the solution and solid states were investigated and compared with those of **1–3** (Fig. 1). These results indicated that naphthoquinone pigments exhibit characteristic colours in both solution and solid states, which depending on the heteroarylthio unit. Notably, although these pigment molecules were achiral, chirality was observed in the solid state of **3**.

2. Results and discussion

Pigments **1–4** were synthesized by the same method as that reported previously for 2-methyl-3-(4-chlorophenylthio)-1,4-naphthalenedione.^{3a} When 2,3-epoxy-2-methyl-1,4-naphthoquinone was treated with 1-methyl-1H-imidazole-2-thiol

* Corresponding author.

E-mail address: y-imai@apch.kindai.ac.jp (Y. Imai).

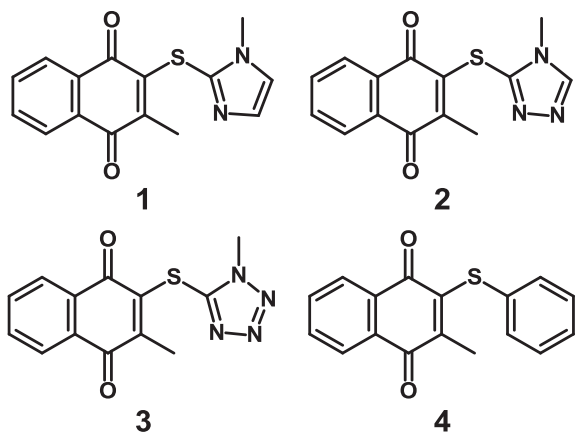
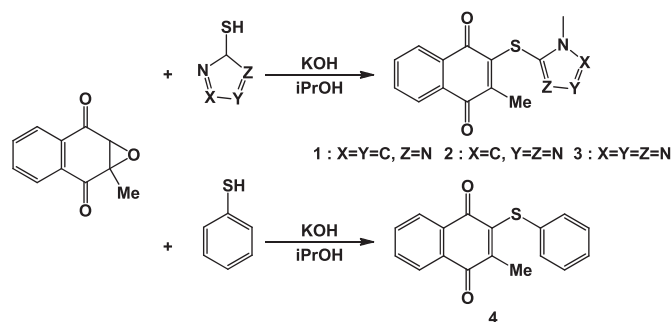


Fig. 1. Naphthoquinone-based heterocyclic pigments **1–3** and naphthoquinone pigment **4**.



Scheme 1. Syntheses of pigments **1–4**.

in a potassium hydroxide solution (0.15%), **1** was obtained in 63% yield. Similarly, pigments **2–4**^{3b} were obtained in 22%, 60%, and 73% yields using 4-methyl-4H-1,2,4-triazole-3-thiol, 1-methyl-1H-tetrazole-5-thiol, and benzenethiol, pigments, respectively (Scheme 1).

First, to investigate the colour of these pigments in the solution state, **1–4** were dissolved in chloroform (CHCl₃) (Fig. 2). Interestingly, although pigment **4**, comprising a simple phenylthio unit, exhibited orange colour in CHCl₃, the colours of **1–3** in CHCl₃ appeared to be different from that of **4** and dramatically changed with the heteroarylthio units in **1–3**. With increasing number of nitrogen atoms (*n*) in the heteroaromatic ring, the solution colour gradually became lighter: brown-red for **1** (*n* = 2), light orange for **2** (*n* = 3), and light green for **3** (*n* = 4).

Fig. 3 shows the UV–Vis absorption spectra of **1–4** in CHCl₃. As expected, the spectra showed markedly different behaviour. As the number of nitrogen atoms in the heteroaromatic ring (*n*) increased,

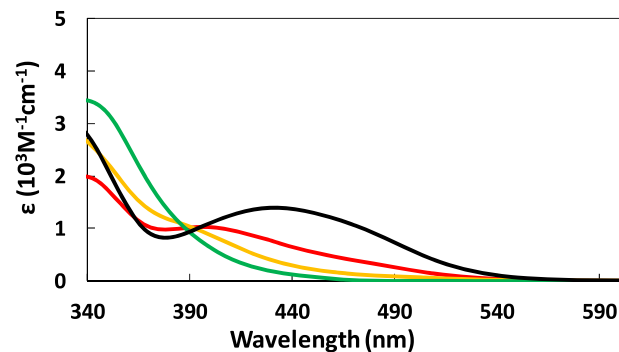


Fig. 3. UV–Vis absorption spectra of **1** (red), **2** (orange), **3** (green), and **4** (black) (1.0×10^{-4} M) in chloroform.

the intensity of the absorbance around 440 nm gradually decreased, with a red line for **1** (*n* = 2), an orange line for **2** (*n* = 3), and a green line for **3** (*n* = 4). These UV–Vis absorption spectra of **1–4** were in agreement with their corresponding solution colours.

To investigate the origin of these pigment colours in CHCl₃, the theoretical equilibrium structures, HOMO and LUMO orbitals of **1–3** in chloroform (Fig. 4), and HOMO–LUMO gaps (Table 1) were calculated using the B3LYP functional⁴ with the cc-pVDZ basis set⁵ using the program Gaussian 03.⁶ The theoretical equilibrium structures of **1–3** are similar: the calculated torsion angles were $\pm 134.2^\circ$ [C(3)–C(2)–S(12)–C(13)] for **1**, $\pm 134.4^\circ$ [C(3)–C(2)–S(12)–C(13)] for **2**, and $\pm 133.4^\circ$ [C(3)–C(2)–S(12)–C(13)] for **3** (Fig. 4).

The HOMO–LUMO gaps calculated for **1–3** are quite different from each other (Table 1). The molecules with the more nitrogen atoms (*n*) in the heteroaromatic ring have the larger HOMO–LUMO gaps: **1** (2.89 eV, *n* = 2) < **2** (3.37 eV, *n* = 3) < **3** (3.56 eV, *n* = 4). This tendency is consistent with the results obtained for the solution colour and UV–Vis absorption spectra, as the molecules with the smaller HOMO–LUMO gap have the longer-wavelength absorption edges. The difference in the HOMO energy of **1–3** was large, compared with that in the LUMO energy of them. As seen in Fig. 4, the HOMO orbitals of **1–3** mainly populate on heterocyclic rings, while their LUMO orbitals mainly populate on naphthoquinone rings. Hence, the colours of **1–3** in the solution state reflect the difference in the HOMO energy, depending on the type of heteroaromatic units.

Next, to investigate the colour of these pigments in the solid state, the crystallization of **1–4** from methanol was carried out. Methanolic solutions of **1–4** were allowed to stand at room temperature. After a few days, large amounts of coloured powders were obtained. Solids of all pigments did not contain methanol, such as those of methanol. Interestingly, the different colours observed for

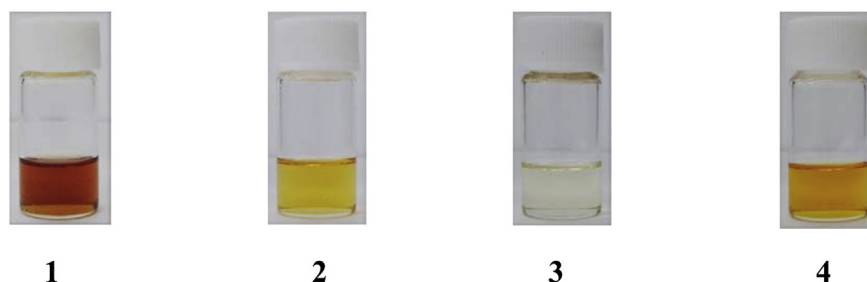


Fig. 2. Photographs of naphthoquinone-based heterocyclic pigments **1–3** and naphthoquinone pigment **4** (1.0×10^{-3} M) in chloroform.

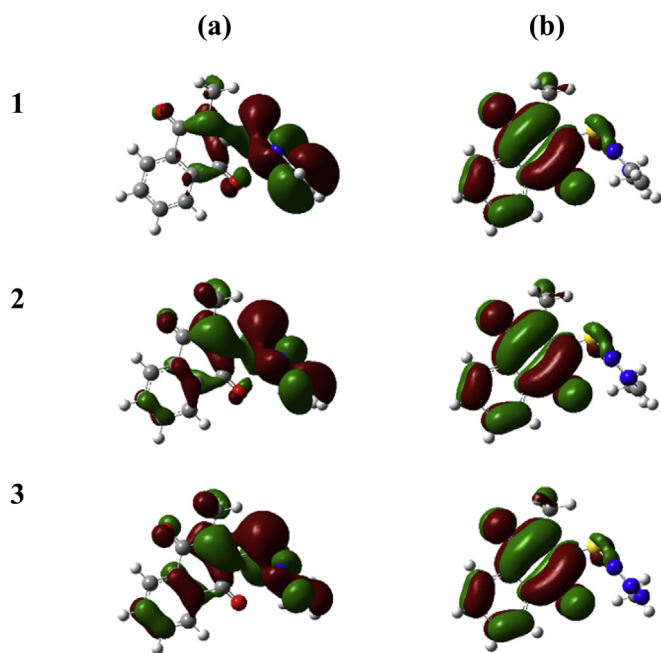


Fig. 4. Theoretically calculated (a) HOMO and (b) LUMO orbitals in pigments 1–3.

Table 1
Theoretically calculated HOMO and LUMO energies of 1–4.

Pigment	HOMO [eV]	LUMO [eV]	HOMO–LUMO Gap [eV]
1	–6.13	–3.24	2.89
2	–6.69	–3.32	3.37
3	–6.99	–3.43	3.56
4	–6.28	–3.20	3.08

pigment 1–3 in chloroform were also seen in the solid state: red/brown for 1, yellow/brown for 2, yellow for 3, and orange for 4 (Fig. 5).

Fig. 6 shows the solid-state diffuse-reflectance spectra (DRS) of 1–4. As expected, markedly different solid-state DRS were observed for 1–3. With increasing numbers of nitrogen atoms in the heteroaromatic ring (n), the absorption edges gradually shifted to short wavelength, with absorption edges of 550 nm for 1 ($n = 2$), 470 nm for 2 ($n = 3$), and 410 nm for 3 ($n = 4$). The DRS and UV–Vis absorption spectra also showed good agreement.

To study the thermal stability of 1–3, TG analyses of 1–4 were employed (Fig. ESI-1). Unfortunately, the pigments 1–3 with the nitrogen atoms in the heteroaromatic ring have the lower thermal stability (20 °C or more) than the pigment 4 without the nitrogen atom in the aromatic ring.

In addition, 1–3 exhibited different solid-state optical properties depending on the heteroarylthio unit. The crystallization of pigments 1–4 from a methanol solution was attempted to investigate

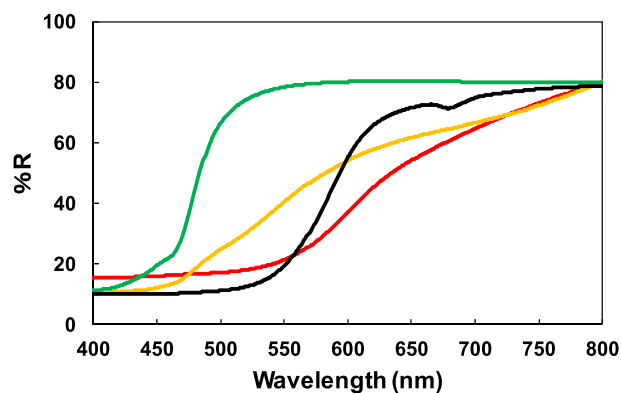


Fig. 6. Diffuse-reflectance spectra (DRS) of 1 (red), 2 (orange), 3 (green), and 4 (black).

their X-ray crystal structures. Good-quality coloured crystals of 3 and 4 were obtained, which were used for X-ray crystallographic analysis.

Fig. 7 shows the X-ray crystallographic structure of 3. Interestingly, this crystal belonged to the chiral space group $P2_12_12_1$. That is, although 3 was an achiral molecule, the crystals of 3 exhibited chirality.

Solid 3 exhibited an intramolecular hydrogen bond (indicated by black arrow A in Fig. 7a, 3.08 Å ($C\cdots S$)).⁷ The torsion angle was $+141.7^\circ$ ($C(3)–C(2)–S(12)–C(13)$), which shifted from the vertical axis (Fig. 7a). In one crystal of 3, all heteroaromatic rings were inclined in the same direction with respect to the naphthalenedione ring. That is, one-handedness was observed in the crystals of 3, making achiral 3 exhibit optical chirality in the solid state. A two-dimensional (2D)-layered network structure was formed (indicated by the red dotted rectangle in Fig. 7b and c) along the a - and b -axes via $CH–\pi$ intermolecular interactions between the methyl group on the naphthoquinone ring and the naphthoquinone ring (indicated by the red arrow B and blue arrow C in Fig. 7b and c, 3.47 and 3.44 Å ($C\cdots\pi$), respectively), and intermolecular hydrogen bonds between hydrogen (H) atom on the naphthoquinone ring and the C=O unit on the naphthoquinone ring or the N atom on the (1-methyl-1H-tetrazol-5-yl)thio ring (indicated by the purple arrow D and orange arrow E in Fig. 7b and c, 3.23 Å ($C\cdots O$) and 3.31 Å ($C\cdots N$), respectively).⁷ Crystal structure of 3 was formed by the self-assembly of this 2D-layered network structure without major interactions.⁷

Fig. 8 shows the crystal structures of 4, which did not contain the crystallization solvent. In contrast to 3, 4 belonged to the achiral space group $P2_1/c$, with torsion angles of $\pm 140.9^\circ$ ($C(3)–C(2)–S(12)–C(13)$), and it exhibited an intramolecular hydrogen bond (indicated by the black arrow A in Fig. 8a, 3.09 Å ($C\cdots S$)).⁷

A 1D columnar network structure was formed by 4 (Fig. 8b, shown by the red dotted circle in Fig. 8c) along the a -axis via $CH–\pi$ intermolecular interactions between the methyl group on the naphthoquinone ring and the naphthoquinone ring (indicated by

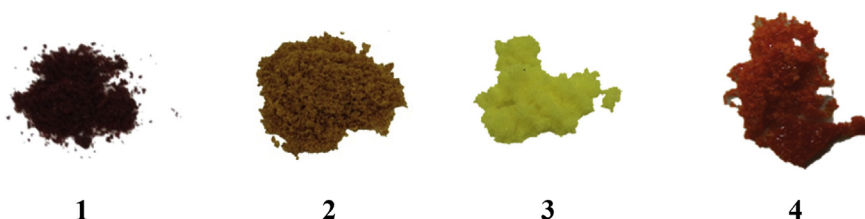


Fig. 5. Images of powders of naphthoquinone-based heterocyclic pigments 1–3 and naphthoquinone pigment 4.

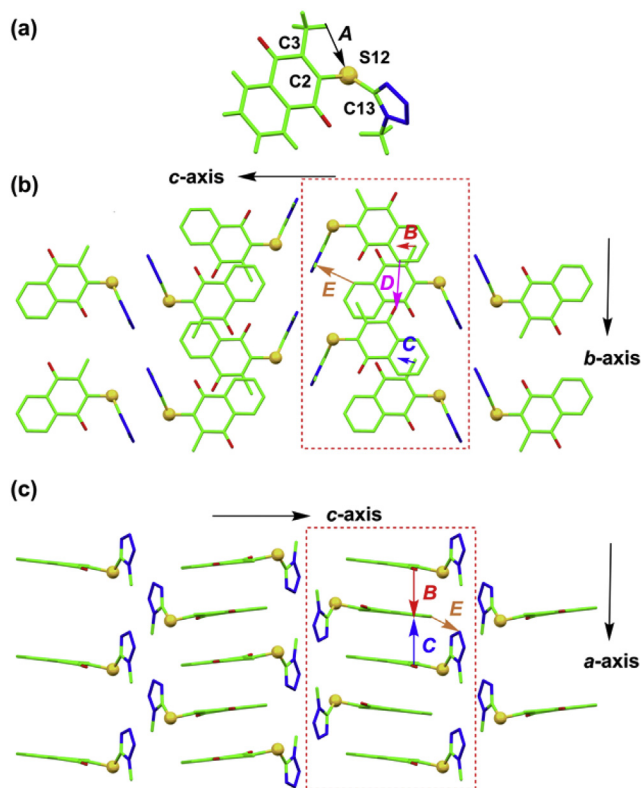


Fig. 7. Crystal structures of **3**. Oxygen, sulfur, and nitrogen atoms are denoted as red, orange, and blue, respectively. (a) Structure of the extracted single molecule **3**. (b) Packing structure observed along the *a*-axis. (c) Packing structure observed along the *b*-axis. Black *A*, purple *D*, and orange *E* arrows indicate hydrogen bonds. Red *B* and blue *C* arrows indicate CH– π interactions. The red dotted rectangle indicates a 2D-layered network structure.

the red arrow *B* and blue arrow *C* in Fig. 8b, 3.50 and 3.53 Å (C \cdots π), respectively) and an intermolecular hydrogen bond between the H atom on the phenylthio ring and the C=O unit on the naphthoquinone ring (indicated by the purple arrow *D* in Fig. 8c, 3.27 Å (C \cdots O)).⁷ The achiral crystal of **4** was formed by the self-assembly of this 1D columnar network structure via intercolumnar hydrogen

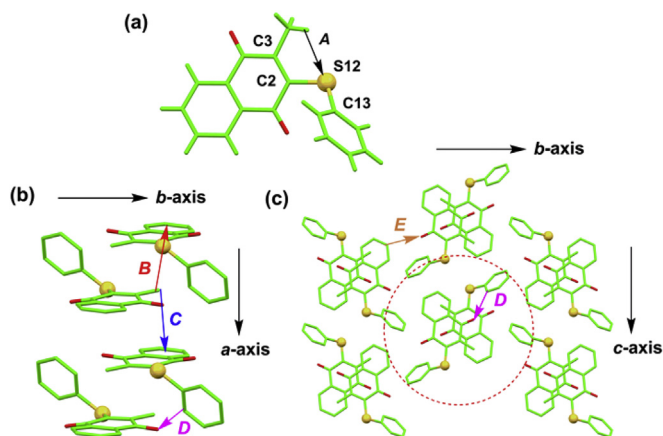


Fig. 8. Crystal structures of **4**. Oxygen and sulfur atoms are shown in red and orange, respectively. (a) Structure of the extracted single molecule **4**. (b) Structure of the 1D columnar network structure along the *a*-axis. (c) Packing structure observed along the *a*-axis. Black *A*, purple *D*, and orange *E* arrows indicate hydrogen bonds. Red *B* and blue *C* arrows indicate CH– π interactions. Red dotted circle shows a 1D columnar network structure.

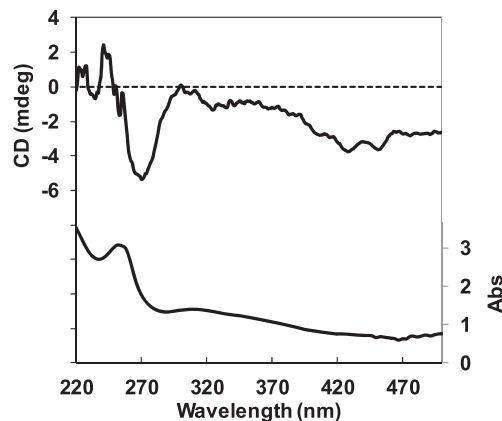


Fig. 9. Solid-state CD and absorption spectra of crystal **3** (KBr pellet).

bonds between a H atom on the naphthoquinone ring and the C=O unit on the naphthoquinone ring (indicated by the orange arrow *E* in Fig. 8c, 3.42 Å (C \cdots O)).⁷

A comparison of the crystal structures and DRS for crystals **3** and **4** showed the presence of small and similar stacking areas between the naphthoquinone units in **3** and **4** (Figs. 7c and 8c), although with different colours and DRS spectra. In addition, the solid and solution-state colours (or DRS and UV–Vis absorption spectra) were similar, indicating that the different colours observed for **1–3** in the crystalline state are probably related to the HOMO–LUMO gaps of single pigment molecules, not depend on the different packing arrangements of pigment molecules, which is the same inference obtained from the solution-state behaviours of **1–3**.

Finally, to investigate the solid-state chiroptical properties of chiral crystal **3**, the circular dichroism (CD) spectrum of the obtained chiral crystals was recorded using a KBr pellet. Fig. 9 shows the solid-state CD and absorption spectra of **3**. Although pigment **3** was an achiral molecule, a clear CD signal was observed as expected.

Peaks corresponding to the naphthoquinone unit were observed between 320 and 470 nm in the CD spectrum. The circular anisotropy factors ($|g_{CD}|$) of the main Cotton band ($\lambda_{CD} = 428$ and 451 nm) were $\sim 1.52 \times 10^{-4}$ and 1.65×10^{-4} , respectively, confirming that achiral pigment **3** induces chirality in the solid state.

3. Conclusion

Three novel naphthoquinone-based heterocyclic pigments were successfully prepared. Depending on the heterocyclic ring, different optical properties were observed. In particular, depending on the heteroarylthio unit, these pigments exhibited characteristic colours in both solution and solid states. Notably, chirality was successfully detected in the solid state for the achiral pigment containing the 1-methyl-1H-tetrazol-5-yl ring. We believe that the study results will be useful for the exploration and design of several novel functional organic pigments that exhibit multiple optical properties.

4. Experimental section

4.1. Materials

The solvent used for crystallization and measurement of optical properties was purchased from Wako Pure Chemical Industries (Osaka, Japan).

4.2. Synthesis of 2-methyl-3-(1-methyl-1H-imidazol-2-yl)thio-1,4-naphthalenedione (**1**)

Pigments **1–4** were prepared by the same method as that reported previously for 2-methyl-3-(4-chlorophenylthio)-1,4-naphthalenedione.³ First, 2,3-epoxy-2-methyl-1,4-naphthoquinone (94 mg, 0.50 mmol) and 2-mercapto-1-methylimidazole (57 mg, 0.50 mmol) were dissolved in isopropanol (30 mL). Second, a potassium hydroxide (0.15%; 0.050 mL) solution was added to the isopropanol solution, and the reaction mixture was stirred at room temperature for 4 h. Next, the solvent was evaporated under vacuum, and the residue was dissolved in dichloromethane (100 mL). The resultant solution was washed with brine, dried over MgSO₄, and evaporated under vacuum, affording a crude naphthoquinone compound. Pigment **1** was purified by column chromatography (SiO₂, chloroform–tetrahydrofuran, 4:1) in 63% yield. ¹H NMR data of **1**: δ_H (400 MHz, CDCl₃) δ = 2.43 (s, 3H), 3.91 (s, 3H), 7.05 (s, 2H), 7.62–7.70 (m, 2H), 7.92 (d, *J* = 7.6 Hz, 1H), 8.08 (d, *J* = 6.8 Hz, 1H). ¹³C NMR data of **1**: δ_C (100 MHz, CDCl₃) 15.2, 34.4, 123.3, 126.7, 126.8, 129.8, 131.9, 132.3, 133.5, 133.8, 136.9, 143.5, 147.3, 180.3, 182.5. M.p. of **1**: 121.9–122.7 °C (from MeOH).

4.3. Synthesis of 2-methyl-3-(4-methyl-4H-1,2,4-triazol-3-yl)thio-1,4-naphthalenedione (**2**)

2,3-Epoxy-2-methyl-1,4-naphthoquinone (94 mg, 0.50 mmol) and 3-mercapto-4-methyl-4H-1,2,4-triazole (58 mg, 0.50 mmol) were dissolved in isopropanol (40 mL). Then, a potassium hydroxide (0.15%; 0.050 mL) solution was added to the isopropanol solution, and the reaction mixture was stirred at room temperature for 15 h. Next, the solvent was evaporated under vacuum, and the residue was dissolved in dichloromethane (100 mL). The resultant solution was washed with brine, dried over MgSO₄, and evaporated under vacuum, affording a crude naphthoquinone compound. Pigment **2** was purified by column chromatography (SiO₂, acetone–hexane, 1:3) in 22% yield. ¹H NMR data of **2**: δ_H (400 MHz, CDCl₃) 2.54 (s, 3H), 3.95 (s, 3H), 7.66–7.71 (m, 2H), 7.88–7.90 (dd, *J* = 1.2, 7.6 Hz, 1H), 8.08–8.11 (dd, *J* = 1.2, 7.6 Hz, 1H), 8.25 (s, 1H). ¹³C NMR data of **2**: δ_C (100 MHz, CDCl₃) 15.8, 34.2, 125.5, 126.8, 127.0, 131.8, 132.0, 133.8, 134.0, 142.1, 145.6, 149.0, 179.8, 182.3. M.p. of **2**: 124.2–126.0 °C (from MeOH).

4.4. Synthesis of 2-methyl-3-(1-methyl-1H-tetrazol-5-yl)thio-1,4-naphthalenedione (**3**)

2,3-Epoxy-2-methyl-1,4-naphthoquinone (94 mg, 0.50 mmol) and 5-mercapto-1-methyltetrazole (58 mg, 0.50 mmol) were dissolved in isopropanol (30 mL). A potassium hydroxide (0.15%; 0.075 mL) solution was added to the isopropanol solution, and the reaction mixture was stirred at room temperature for 8 h. After filtration and washing, pigment **3** was obtained in 60% yield by filtration. ¹H NMR data of **3**: δ_H (400 MHz, CDCl₃) 2.56 (s, 3H), 4.28 (s, 3H), 7.69–7.77 (m, 2H), 7.92–7.95 (m, 1H), 8.11–8.13 (dd, *J* = 1.6, 7.2 Hz, 1H). ¹³C NMR data of **3**: δ_C (100 MHz, CDCl₃) 16.3, 34.5, 127.0, 127.2, 131.7, 131.9, 134.0, 134.3, 139.8, 150.4, 151.3, 179.1, and 182.2. M.p. of **3**: 153.4–154.3 °C (from MeOH).

4.5. Synthesis of 2-methyl-3-phenylthio-1,4-naphthalenedione (**4**)

2,3-Epoxy-2-methyl-1,4-naphthoquinone (94 mg, 0.50 mmol) and benzenethiol (0.05 mL, 0.49 mmol) were dissolved in isopropanol (30 mL). Then, a potassium hydroxide (0.15%; 0.025 mL) solution was added to the isopropanol solution, and the reaction mixture was stirred at room temperature for 3 h. Next, the solvent was evaporated under vacuum, and the residue was dissolved in

dichloromethane (100 mL). The resultant solution was washed with brine, dried over MgSO₄, and evaporated under vacuum, affording a crude naphthoquinone compound. Pigment **4** was purified by column chromatography (SiO₂, benzene) in 80% yields. ¹H NMR data of **4**: δ_H (400 MHz, CDCl₃) 2.35 (s, 1H), 7.23–7.31 (m, 3H), 7.37 (d, *J* = 6.4 Hz, 2H), 7.67–7.74 (m, 2H), 8.03 (d, *J* = 6.8 Hz, 1H), 8.11 (d, *J* = 6.8 Hz, 1H). ¹³C NMR data of **4**: δ_C (100 MHz, CDCl₃) 16.0, 126.7, 127.1, 127.4, 129.2, 130.6, 132.1, 132.6, 133.7, 133.7, 134.1, 145.5, 149.2, 180.5, and 183.1. M.p. of **4**: 113.6–114.4 °C (from MeOH).

4.6. Characterisation

¹H and ¹³C NMR spectra were recorded on a JEOL JNM-AL400 spectrometer using tetramethylsilane as the internal standard. Circular dichroism (CD) and absorption spectra were measured using a Jasco J-800KCM spectrophotometer. Melting points were measured using a Yanagimoto MP-S3 micro-melting point apparatus. Diffuse-reflectance spectra (DRS) and UV–Vis absorption spectra were measured with a Jasco V-670 spectrometer. X-ray diffraction (XRD) data for a single crystal of **3** were measured on a RIGAKU SATURN 70R system. XRD data for a single crystal of **4** were obtained using a BRUKER APEX instrument. The crystal structures were solved by direct methods⁸ and refined by full-matrix least-squares method using SHELXL97.⁸ The diagrams were prepared using PLATON.⁹ Absorption corrections for **3** were performed using the multi-scan program, while those for **4** were performed using SADABS.¹⁰ Nonhydrogen atoms were refined with anisotropic displacement parameters, and hydrogen atoms were included in the models at their calculated positions in the riding-model approximation. Crystallographic data for **3**: C₁₃H₁₀N₄O₂S, *M* = 286.31, orthorhombic space group *P*2₁2₁2₁, *a* = 6.8213(14) Å, *b* = 8.0009(17) Å, *c* = 23.100(5) Å, *V* = 1260.7(5) Å³, *Z* = 4, *D*_c = 1.508 g/cm³, μ (Mo *K*α) = 0.264 mm⁻¹, 9437 reflections measured, 2874 unique, final *R*(*F*²) = 0.0322, using 4651 reflections with *I* > 2.0 σ(*I*), *R* (all data) = 0.0328, *T* = 293 K, CCDC 1513021. Crystallographic data for **4**: C₁₇H₁₂O₂S, *M* = 280.33, monoclinic space group *P*2₁/*c*, *a* = 6.9608(7) Å, *b* = 19.256(2) Å, *c* = 10.2001(2) Å, β = 104.222(2)°, *V* = 1325.3(2) Å³, *Z* = 4, *D*_c = 1.405 g/cm³, μ (Mo *K*α) = 0.241 mm⁻¹, 8021 reflections measured, 3003 unique, final *R*(*F*²) = 0.0566, using 2656 reflections with *I* > 2.0 σ(*I*), *R*(all data) = 0.0627, *T* = 115(2) K, CCDC 1513020. Crystallographic data can be obtained free of charge via <http://www.ccdc.cam.ac.uk/conts/retrieving.html> (or from the Cambridge Crystallographic Data Centre, 12, Union Road, Cambridge CB21EZ, UK; fax: +44 1223 336 033; deposit@ccdc.cam.ac.uk).

4.7. Theoretical calculations

Theoretical calculations were performed with the GAUSSIAN 09 program.⁶ The geometries of **1–4** were optimized by the hybrid density functional theory (B3LYP functional)⁴ using the cc-pVDZ basis set.⁵

4.8. Measurement of thermogravimetry (TG)

Simultaneous thermogravimetric (TG) curves were obtained using Thermo plus EVOII TG-DTA. Approximately 3–7 mg samples were run in aluminum sample pans under an air atmosphere. The scans were started at 25 °C and continued at 10 °C min⁻¹ until an acceptable baseline could be obtained post transition. The temperature was calibrated using an alumina standard material. The performance of the mass balance was confirmed using a certified weight set.

Acknowledgements

This study was supported by a Grant-in-Aid for Scientific Research (no. 15K05489) from MEXT/JSPS and the MEXT-Supported Program for the Scleroderma Research Foundation at Private Universities (2014–2018). X-ray crystallographic analyses were supported by Dr. Kyohei Sato (Tokyo University of Science).

Appendix A. Supplementary data

Supplementary data related to this article can be found at <http://dx.doi.org/10.1016/j.tet.2017.02.053>.

References

- (a) Chu KY, Griffiths J. *J Chem Soc Perkin Trans.* 1979;1:696–701;
(b) Karci F, Ertan N. *Color Technol.* 2005;121:153–157;
(c) Yoshida S, Kubo H, Saika T, Katsumura S. *Chem Lett.* 1996;139–140;
(d) Parisot D, Devys M, Barbier M. *Microbios.* 1990;64:31–47;
(e) Chen X, Yang L, Oppenheim JJ, Howard OM. *Z Phytother Res.* 2002;16:199–209;
(f) Marjit Singh W, Baruah JB. *J Mol Struct.* 2009;931:82–86;
- (g) Jali BR, Baruah JB. *Cryst Growth Des.* 2012;12:3114–3122 (and references cited therein).
- (a) Imai Y, Kinuta T, Nagasaki K, et al. *CrystEngComm.* 2009;11:1223–1225;
(b) Kinuta T, Sato T, Harada T, et al. *J Mol Struct.* 2010;982:16–21;
(c) Kinuta T, Sato T, Tajima N, Matsubara Y, Miyazawa M, Imai Y. *CrystEngComm.* 2012;14:1016–1020;
(d) Akiyama T, Inoue H, Tajima N, Kuroda R, Imai Y. *Org Biomol Chem.* 2014;12:7965–7970;
(e) Akiyama H, Sako A, Tajima N, Shizuma M, Kuroda R, Imai Y. *Tetrahedron.* 2016;72:2109–2115.
- (a) Yotsumoto E, Inoue T, Wakabayashi T, et al. *J Mol Struct.* 2014;1056:189–193;
(b) Mecklenburg S, Shaaban S, Ba LA, et al. *Org Biomol Chem.* 2009;7:4753–4762.
- Becke AD. *J Chem Phys.* 1993;98:5648–5652.
- (a) Dunning Jr TH. *J Chem Phys.* 1989;90:1007–1023;
(b) Woon DE, Dunning Jr TH. *J Chem Phys.* 1993;98:1358–1371.
- Frisch MJ, Trucks GW, Schlegel HB, et al. *GAUSSIAN 09 (Rev. D.01)*. Wallingford CT: Gaussian, Inc.; 2013.
- It is determined by PLATON geometry calculation.
- Sheldrick GM. *Acta Crystallogr Sect A.* 2008;64:112–122.
- Spek AL. *PLATON, a Multipurpose Crystallographic Tool*. Utrecht, Netherlands: Utrecht University; 2010.
- Sheldrick GM. *SADABS, Program for Empirical Absorption Correction of Area Detector Data*. Germany: University of Göttingen; 1996.